Bulletin of the National Research Centre

RESEARCH

Open Access

In silico studies on the interaction of four cytotoxic compounds with angiogenesis target protein HIF-1α and human androgen receptor and their ADMET properties

Jean-Paul Koto-Te-Nyiwa Ngbolua[1,2*], Jason T. Kilembe[3], Aristote Matondo[3], Colette Masengo Ashande[1], Janvier Mukiza[4], Célestin Mudogo Nzanzu[5], Fatiany Pierre Ruphin[6], Robijaona Baholy[7], Pius T. Mpiana[3] and Virima Mudogo[3]

Abstract

Background: Cancer is a significant public health problem worldwide and constitutes the second leading cause of death after cardiovascular disease. This study was thus designed to identify new natural compounds from Malagasy medicinal plants traditionally used to treat cancer.

Methods: In silico analyses by molecular docking to model ligand–protein interactions, and by SwissADME and ADMET webservers to establish the pharmacokinetic profile of the four investigated compounds in interaction with the angiogenesis target protein HIF-1α/breast cancer (PDB ID: 3KCX) and human androgen receptor/prostate cancer (PDB ID: 1E3G) were performed.

Results: The docking results show that the HIF-1α receptor has the best binding energy when it interacts with compound **1** (1′,4-dihydroxy-2,3′-dimethyl-1,2′-binapthyl-5,5′,8,8′-tetraone: − 8.49 kcal/mol) followed by compound **3** [(E)-5,6-dimethyl-2-(2-methyl-3-(prop-1-enyl)phenyl)-2H-chromene: -8.43 kcal/mol], compound **2** (6′-ethoxy-1′3′-dihydroxy-4,6-dimethyl-1,2′-binaphthyl-2,5′,8,8′-tetraone: − 7.80 kcal/mol) and compound **4** (methyl 10-hydroxy-2,4a,6a,9,12b,14a-hexamethyl-11-oxo-1,2,3,4,4a,5,6,6a,11,12b,13,14,14a,14b-tetradecahydropicene-2-carboxylate: − 7.63 kcal/mol). The receptor 1E3G displayed poor binding affinity energy to all tested compounds with energy value above − 11.99 kcal/mol (co-crystal). Based on the H-bonding interaction, ligands **1** and **2** displayed a good pharmacophore profiles to both protein targets 3KCX and 1E3G. Ligand **3** does not interact with the selected receptors via hydrogen bonds. The pharmacokinetic profile of these phyto-compounds revealed that they are orally active and safe. They were isolated and their chemical structures were elucidated previously by our team using chromatographic and spectroscopic techniques (LC/MS/NMR).

Conclusions: The ligands **1** and **2** can be considered as hits since in addition to their thermodynamic stability with the receptors; they presented a good pharmacokinetic profile and could thus be useful as an alternative therapy in breast and prostate cancer. This study offers a strong potential in developing new, cost-effective, and safe plant-based natural drugs against cancer.

*Correspondence: jpngbolua@unikin.ac.cd
[1] Department of Basic Sciences, Faculty of Medicine, University of Gbado-Lite, Gbado-Lite, Nord-Ubangi Province, Democratic Republic of the Congo
Full list of author information is available at the end of the article

Keywords: Evidence-based medicine, Structural molecular biology, Chemo-informatics, Cancer, Madagascar

Background

Cancer is a significant public health problem worldwide and constitutes the second leading cause of death after cardiovascular disease. Because of the serious side effects of both chemo-and radiation therapies, many patients seek alternative and complementary treatment methods. Several anti-cancer agents derived from plant species (Taxol, Camptothecin, Topotecan, etc., and their derivatives) are in clinical use or preclinical development (flavopiridol, silvestrol, betulinic acid, etc.) (Tshibangu et al. 2016a, b). Folk medicine's role in the treatment and management of cancer has recently been reported in the literature (Tshibangu et al. 2016a, b; Ngbolua et al. 2018). Indeed, medicinal plants are an essential source of secondary metabolites used as therapeutic agents against cancer. Medicinal plant species, especially those applied in traditional medicine, have attracted significant attention because they include bioactive compounds that could develop legal or approved drugs against several diseases with no or minimal side effects (Iteku et al. 2019; Tshilanda et al. 2019). According to a WHO report, more than 80% of the population in developing countries uses traditional medicine to solve the primary health problem (Ngbolua et al. 2011a, b). As one of the hotspots of plant biodiversity in the world, Madagascar could play a vital role in the research and development of new anticancer agents from its flora. This study aimed to examine the interaction of four cytotoxic compounds isolated from Madagascar endemic medicinal plants *Diospyros quercina* and *Salacia leptoclada* with both angiogenesis target protein HIF-1α and human androgen receptor (HAR) by evaluating binding affinity energy of formed complex and defining the amino residues involved in such interaction. These compounds were scientifically validated in vitro on P388 cell lines model, and they have an $IC_{50} < 1$ µg/mL (Fatiany et al. 2013, 2014). These two medicinal plants are widely used in southern Madagascar to treat malaria and cancer. Apart from our work, no pharmacobiological research has been initiated to date on these four secondary metabolites. The molecular docking strategy was based on the hypothesis that Malagasy-derived phytochemicals can interfere with HIF-1α pathways or androgen activity thus resulting in inhibition of cancer initiation and progression. The protein–ligand interactions were carried out using molecular docking AutoDock Vina in PyRx 0.8 software package to investigate the binding affinity of selected secondary metabolites against HIF-1α and AR. The three-dimensional (3D) structure of HIF-1α and AR was retrieved from Protein Data Bank and docked with 3D Pubchem structures of selected phytochemicals using Argus Lab. Molecular docking and drug-likeness studies were made using ADMET properties; simultaneously, Lipinski's rule of five was performed for the selected phytochemicals to evaluate their binding affinity activity and toxicity profile in silico.

The interest of the present study is obvious as it will allow to scientifically validating the use of plants in traditional medicine for the treatment of cancer, and also, the selected compounds could later serve as a starting point for a galenic formulation or as precursors for an industrial scale chemical synthesis. In addition, these data will allow the in vivo antitumor effects evaluation of these isolated compounds on Ehrlich ascites carcinoma cells model by evaluating both the mean survival time and the percent increase in life span of mice (Nirmala et al. 2022).

Methods

Molecular docking studies

Protein preparation

The crystal structures of both HIF-1α (PDB ID: 3KCX) and HAR (PDB ID: 1E3G) were retrieved from the Protein Data Bank and imported into chimera for visualizing the binding domain and identifying the amino acids in the binding pocket. The survey of the inhibitor binding site was carried out with the reference of amino acid residues in the binding domain, as previously reported (Anshika et al. 2017; Vidya et al. 2019). The hydrogen atoms were added to the protein in order to correct the ionization and tautomeric states of the amino acid residues. The water molecules and complexes bound to the receptor molecules were removed before the docking. HIF-1α was prepared for docking. Incomplete side chains were replaced using the Drunbrack rotamer library (Shapovalov and Dunbrack 2011). In addition, the protein was subjected to energy minimization by applying the AMBER 14SB force field, and AM1-BCC was used for other residues with a maximum number of 200 steps at a RMS gradient of 0.02. The optimized protein was saved in.pdbqt format and imported to PyRx for molecular docking which was carried out by means of the Autodock Vina virtual screening tool (Trott and Olson 2010).

Generation of ligand dataset

The selected compounds (of which three belongs to the quinone-methide family) were isolated, and their chemical structures were elucidated previously by our team using chromatographic and spectroscopic techniques

(LC/MS/NMR). The cytotoxic effect of pure compounds was confirmed in vitro on P388 cell lines model system [IC_{50} (µg/mL): 0.0175 ± 0.0060 (Compound **1**: *Diospyros quercina*); 0.0895 ± 0.0050 (Compound **2**: *D. quercina*); 1.27 ± 0.07 (Compound **3**: *D. quercina*); 0.041 ± 0.02 (Compound **4**: *Salacia leptoclada*)] (Fatiany et al. 2013, 2014). The chemical structures of these phyto-compounds were drawn using ACD/MarvinSketch (20.9). Figure 1 shows the 2D structure of the sketched compounds. Further ligands were imported into ChemDraw to obtain 3D from 2D. The 3D ligands were optimized using Mercury software by conformer generation. The drug-likeness and ADME properties of the ligand dataset were evaluated with the SwissADME descriptor (Daina et al. 2017).

The structures of ligands (compounds **1–4)** derived from medicinal plants endemic to Madagascar are shown in Fig. 1.

Docking strategy

Autodock Vina and Pyrex were used to generate the bioactive binding poses of ligands dataset in the active site of both HIF-1α and HAR.

The protein coordinates from the bound ligand of 3KCX and 1E3G were used to define the active site. The Scoring function was calculated using the standard protocol of the Lamarckian genetic algorithm (Morris et al. 1998; Selvaraj et al. 2019).

The grid map for docking calculations was centered on the target proteins according to Vidya et al. (2019) and Anshika et al. (2017).

Accelrys Discovery Studio 2019 software was used to model non-bonded polar and hydrophobic contacts in the inhibitor site of both 3KCX and 1E3G. The hit molecules, which showed the expected interactions with the critical amino acids present in the active site of the protein, may show potent antagonist properties toward 3KCX and 1E3G. The three-dimensional crystal structures of the target proteins are displayed in Fig. 2.

The validation of the docking study was performed by re-docking the reference ligand into an appropriate protein cavity. Re-docking is accepted if the root mean square deviation (RMSD) is lower or equal to 2.0 Å (Nissink et al. 2002; Matondo et al. 2020). The RMSD of 0.45 Å was obtained by superposing the ligand poses in the binding site of 1E3G (Fig. 3).

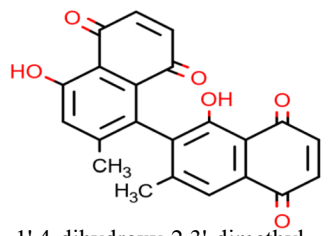

1',4-dihydroxy-2,3'-dimethyl-1,2'-binaphthyl-5,5',8,8'-tetraone

Compound 1 (Fatianone)

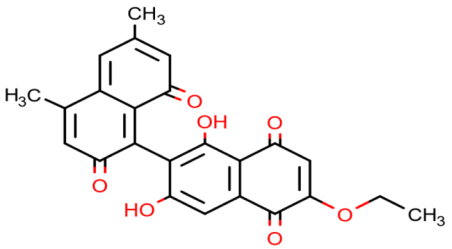

6'-ethoxy-1',3'-dihydroxy-4,6-dimethyl-1,2'-binaphthyl-2,5',8,8'-tetraone

Compound 2 (Robijaonone)

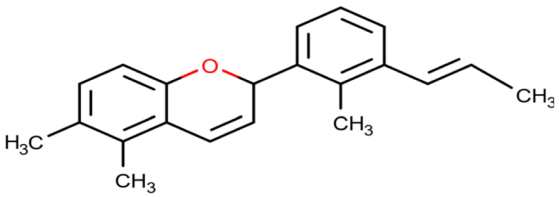

(E)-5,6-dimethyl-2-(2-methyl-3-(prop-1-enyl)phenyl)-2H-chromene

Compound 3

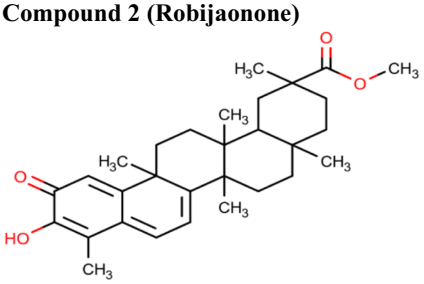

methyl 10-hydroxy-2,4a,6a,9,12b,14a-hexamethyl-11-oxo-1,2,3,4,4a,5,6,6a,11,12b,13,14,14a,14b-tetradecahydropicene-2-carboxylate

Compound 4

Fig. 1 Chemical structure of isolated compounds

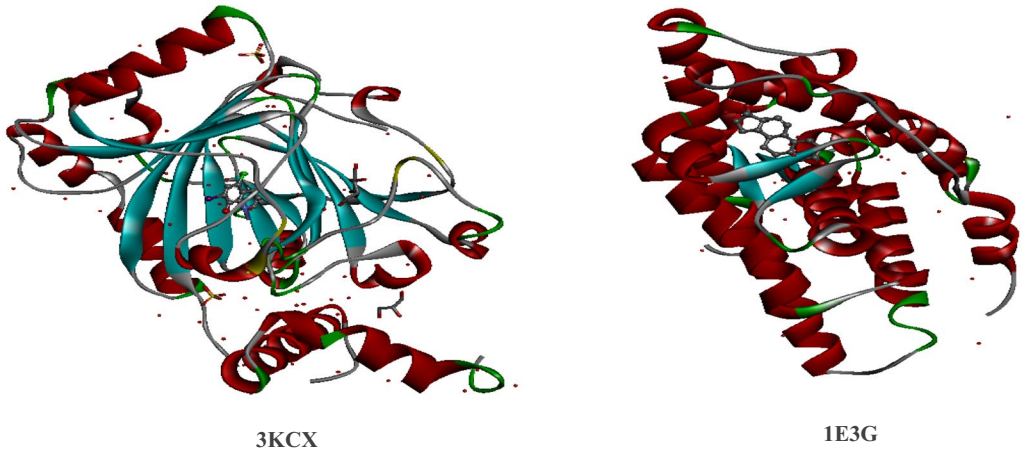

Fig. 2 3D structure of target proteins 3KCX and 1E3G

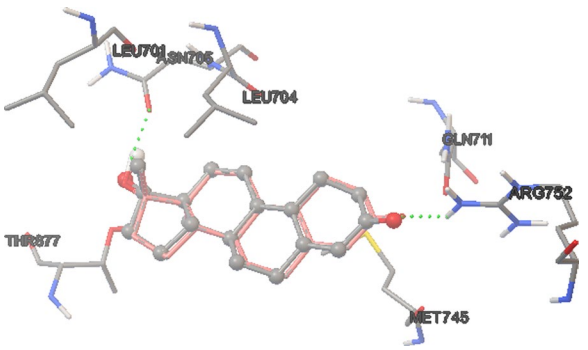

Fig. 3 Superposition of an experimental pose (in red) and a pose derived from docking (in gray)

ADMET profiling

To establish the ADMET profile of four ligands, the in silico prediction of their absorption, distribution, metabolism, excretion, and toxicity was made possible by using bioinformatics resources. The drug-likeness properties were calculated by using the SwissADME online tool. The parameters such as molecular weight (MW), bioavailability score (BioS), number of the rotatable bonds (nRB), hydrogen bond acceptor (HBA), hydrogen bond donor (HBD), molar refractivity (MR), and topological surface area (TSA) were calculated. The assessment of different ADME pharmacokinetic properties along with toxicity was done for the four compounds by using the pkCSM webserver.

Results

Energetics and ligand–protein interactions

Table 1 lists the energetic parameters (binding affinity ΔG, ligand efficiency LE and desolvation energy DE) and the inhibition constant IC of the tested four phytocompounds used in the present study, in the interaction with the main targets involved in the progression of breast cancer (3KCX) and prostate cancer (1E3G).

Concerning the inhibition of the biological activity of the tested compounds, the involvement of the residues of certain so-called key amino acids in hydrogen bonds

Table 1 Binding affinity energies of the tested phytocompounds

Compound	Energetic parameters (Kcal/mol)							
	Receptor PDB ID: 3KCX (Breast cancer)				Receptor PDB ID: 1E3G (Prostate cancer)			
	ΔG	LE	VDW_HB/DE	IC (nM)	*ΔG*	LE	VDW_HB/DE	IC (nM)
1	− 8.49	− 0.30	− 8.82	766.77	− 10.08	− 0.36	− 10.69	40.72
2	− 7.80	0.23	− 8.66	4.63	− 5.88	− 0.19	− 7.01	49.23
3	− 8.43	0.38	− 9.05	666.38	− 9.61	− 0.44	− 10.21	90.29
4	− 7.63	0.22	− 8.33	2.54	− 14.63	0.43	14.07	No
Reference Ligand	− 6.60	− 0.51	− 6.77	− 6.60	− 11.99	− 0.57	12.08	1.63

Threshold energy: − 6.60 kcal/mol (3KCX) or − 11.99 kcal/mol (1E3G)

and hydrophobic interactions is decisive. These amino acids include THR877, MET742, GLN711 and, ARG752 (Table 2).

Table 2 Interacting amino acids of 3KCX and 1E3G in H-bond interactions

Compound	3KCX (breast cancer)		1E3G (prostate cancer)	
	HB	Amino acids	HB	Amino acids
1	3	THR196, HIS199, ASP201	4	THR877, MET742, GLN711, ARG752
2	4	HIS279, ARG238, THR196, ASP201	1	TYR915
3	0		0	
4	3	THR196, SER184, GLN 147		–
PDB ligand	0			0

The 2D representations of interactions of the four investigated phytocompounds with the target receptors 3KCX and 1E3G are depicted in Figs. 4 and 5, respectively.

With regard to the ADMET prediction and drug-likeness prediction, the physicochemical properties and the pharmacokinetic behavior of the 4 ligands were predicted and their results are gathered in Tables 3 and 4, respectively.

Discussion

The docking results show that the HIF-1α receptor has the best binding energy when it interacts with compound **1** (− 8.49 kcal/mol) followed by compound **3** (− 8.43 kcal/mol) and compound **2** (− 7.80 kcal/mol). The desolvation energies are in agreement with the

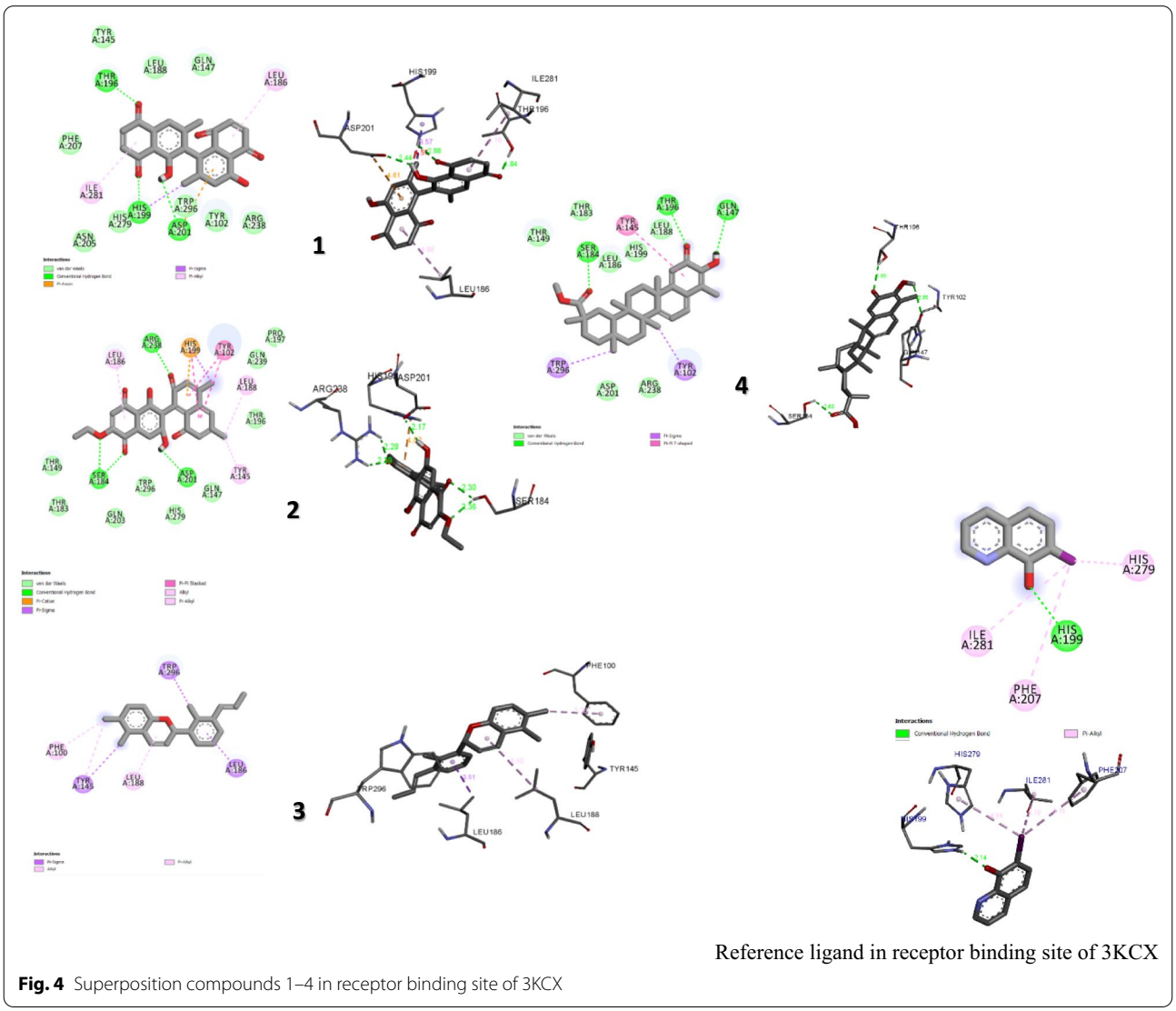

Fig. 4 Superposition compounds 1–4 in receptor binding site of 3KCX

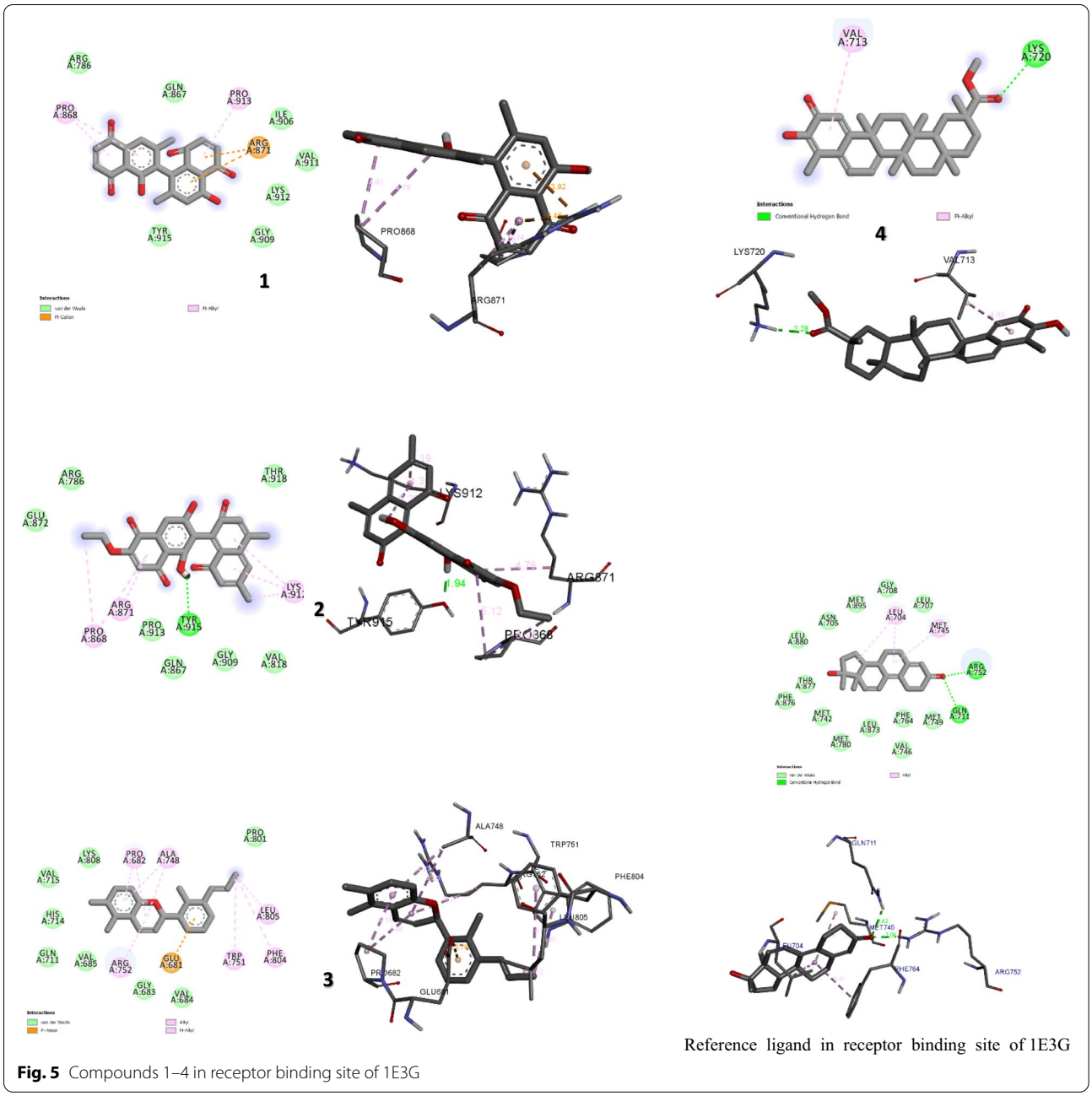

Fig. 5 Compounds 1–4 in receptor binding site of 1E3G

Table 3 Computational parameters of drug-likeness and ADME properties of compounds isolated from Malagasy medicinal plants traditionally used to treat cancer

Compound	MW (Da)	BioS	nRB	Log P	HBD	HBA	TPS (Å^2)	Log S	Log Kp (cm/s)
1	374.34	0.55	1	2.32	2	6	108.74	−4.76	−5.94
2	418.40	0.56	3	2.65	2	7	117.97	−3.80	−7.25
3	290.40	0.55	2	3.95	0	1	9.23	−5.72	−3.78
4	464.64	0.55	2	4.25	1	4	63.60	−6.54	−4.68

MW, molecular weight; BioS, bioavailability score; nRB, number of rotatable bond; Log *P*, partition coefficient; HBD, hydrogen bond donor; HBA, hydrogen bond acceptor; TPS, total polar surface; Log *S*, solubility; Log K_p skin permeation

Table 4 Computational parameters for ADME profile and toxicity risks of compounds isolated from Malagasy medicinal plants traditionally used to treat cancer

Property	Parameters	Compounds			
		1	**2**	**3**	**4**
Absorption	Water solubility(log mol/L)	− 3.803	− 3.671	− 6.596	− 6.131
	Caco2 permeability(log Papp in 10^{-6} cm/s)	1.038	1.283	1.111	0.761
	Intestinal absorption (human) (% Absorbed)	89.82	73.349	98.351	98.371
	Skin Permeability (log Kp)	− 2.968	− 3.179	− 2.202	− 3.04
	P-glycoprotein substrate(Yes/No)	Yes	Yes	No	No
	P-glycoprotein I inhibitor(Yes/No)	Yes	Yes	Yes	Yes
	P-glycoprotein II inhibitor	No	No	No	Yes
Distribution	VDss (human)(log L/kg)	0.032	0.349	1.105	-0.122
	Fraction unbound (human)	0.137	0.128	0	0
	BBB permeability (log BB)	− 0.211	− 0.427	0.749	− 0.104
	CNS permeability (log PS)	− 2.858	− 3.279	− 1.341	− 1.249
Metabolism	CYP2D6 substrate	No	No	No	No
	CYP3A4 substrate	No	No	Yes	Yes
	CYP1A2 inhibitor	No	No	Yes	No
	CYP2C19 inhibitor	No	No	Yes	No
	CYP2C9 inhibitor	No	No	Yes	No
	CYP2D6 inhibitor	No	No	No	No
	CYP3A4 inhibitor	Yes	No	No	No
Excretion	Total clearance	0.398	0.074	0.226	− 0.026
	Renal OCT2 substrate	No	No	Yes	No
Toxicity	AMES toxicity	Yes	No	No	No
	Max. tolerated dose (human)(log mg/kg/day)	− 0.103	− 0.461	0.701	− 0.026
	hERG I inhibitor	No	No	No	No
	hERG II inhibitor	No	No	No	No
	Oral Rat Acute Toxicity (LD50)(mol/kg)	2.228	2.388	2.178	3.054
	Oral Rat Chronic Toxicity (LOAEL)(log mg/kg_bw/day)	1.735	2.133	1.009	2.1
	Hepatotoxicity	Yes	No	No	No
	Skin Sensitization	No	No	No	No
	T. Pyriformis toxicity(log ug/L)	0.389	0.313	1.689	0.333
	Minnow toxicity (log mM)	1.897	0.57	− 1.007	− 1.493

binding energies. Compounds **1** and **3** are so close in terms of stability.

Further, Fig. 4 reveals that both compounds 1 and 2 docked to residues located in the HIF-1α active site with four hydrogen bonds. Compound **2** interacts via its OH and O=C functional groups with active site amino acids HIS279, ARG238, THR196, and ASP201 of the receptor HIF-1α, while compound **1** interacts with active site amino acids ARG238 with its OH group and SER184 with its O=C group. Compound **4** docked to the residues located in the HIF-1α active site with two hydrogen bonds (THR196, SER184).

Surprisingly, no H-bonding interaction occurs in the complex that involves ligand **3** despite its large binding energy (− 8.43 kcal/mol), very close to that of the most stable complex. Such a result was also observed by other previous studies (Tunga et al. 2020; Kasende et al. 2017). However, it is noteworthy to mention that the complex between ligand **3** and the receptor HIF-1α (3KCX) is mainly stabilized by π-π interactions (stacked and T-shaped) and van der Walls interactions that contain a large quantity of dispersion energy. The stabilization of other complexes is strengthened by the π–π, π-cation, π-alkyl, π-sigma, and vdW interactions as well (Mpiana et al. 2020; Matondo et al. 2021).

Overall, modeling of contact shows lipophilic and hydrogen-bonding interactions involving typical hydrophobic and polar amino acid residues which are crucial for the inhibitory interaction of HIF-1α (Vidya et al. 2019). In particular, ASP201 and ARG238 residues play a

significant function in the inhibitory interaction between compounds **1**/**2** and HIF-1α. These key residues are located in the binding site of the HIF-1α protein.

In terms of ligand efficiency, a compound to be selected as a hit should possess a threshold value of 0.3 (Hopkins et al. 2004). All investigated compounds have ligand efficiency greater than the threshold value, except compound **1** (− 0.30 kcal/mol). Nevertheless, there do appear to be situations in which a compound with an inhibitory effect has a LE value lower than the threshold value (Hopkins et al. 2004; Alamri 2020).

Thermodynamically, compounds **1**, **2,** and **3** play a significant role in the inhibition of HIF-1α regarding the interaction energy values of the formed complexes. Recent findings revealed that hypoxia, a condition closely associated with the tumor environment due to the fast growth of cancerous cells, is caused by the lack of adequate blood supply. This condition causes the activation of hypoxia-inducible factor (HIF), a protein transcription factor involved in carcinogenesis, and tumor growth through the up-regulation of genes involved in angiogenesis.

Indeed, in hypoxia conditions, HIF-1 interacts with the positive regulatory sequence or enhancer called hypoxia response element (HER) of the vascular endothelial growth factor (VEGF) gene in order to facilitate the creation of new blood vessels at the tumor level and to answer the energy demand efficiently and therefore of oxygen bound to the anarchic cells proliferation (Gothié and Pouysségur 2002; Pezzuto and Carico 2018).

In relation to the second receptor, 1E3G, the results in Table 1 show that the score values vary between − 10.04 and + 14.38 kcal/mole. The 2D representation of interactions of the 4 ligands with the 1E3G receptor complexes is depicted in Fig. 5. Among the top binding ligands to 1E3G, two potential inhibitors are identified, ligands **1** and **3** with binding energies of − 10.08 and − 9.61 kcal/mole, respectively. These two compounds are also those identified as potential inhibitors for the receptor 3KCX, and have ligand efficiency values lower than the threshold value. For both 3KCX and 1E3G receptors, the weakest complex is obtained with ligand **4.**

Prostate cancer is the second most common malignancy among men all over the world. Its therapy is based on the use of drugs acting as antagonists of hormone receptors against the prostate tissue (Anshika et al. 2017).

Overall, cancer treatment can be performed in various ways, such as surgery, chemotherapy, radiotherapy, immunotherapies, gene therapy, or protein therapy (Siegel et al. 2019). However, on the one hand, the cost of treatment is too high that in low- and middle-income countries, people are unable to support their medical care, and on other hand, most anticancer drugs have several side effects in addition to the drug resistance problem. Currently, the use of plant-based bio-active extracts and phytochemicals is gaining recognition as these have structural diversity, negligible side effects, and bio-availability, as well as exhibit multiple target activities (Ashfaq et al. 2013).

The search for phytochemicals having significant androgen receptor inhibition activity could help the development of new drugs from African plant biodiversity. The results showed that compounds **1, 2** and **3** have significant activity in inhibiting the receptors. The present study therefore reveals that these two phytochemicals could be promising candidates for further evaluation in the prostate cancer prevention or management. In fact, the interaction of these secondary metabolites with androgen receptor could inhibit signaling pathways implicated in the development and progression of prostate cancer especially MAPK and PI3K pathways (Lonergan and Tindall 2011). Further post-docking calculations, namely molecular dynamics simulations (Hollingsworth and Dror 2018) and or MM-PBSA/MM-GBSA (Genheden and Ryde 2015) of four ligand–receptor complexes obtained, should be carried out in near future for confirmation of anti-cancer activities of compounds. However, the three compounds studied in this work belong to the quinone-methide family and several studies have highlighted the anticancer activities of these compounds or even of compounds which include a quinone-methide moity (Dufrasne et al. 2011; Hernandes et al. 2020).

According to threshold energy, a best anti-cancer activity is obtained if the binding energy is above − 6.60 kcal/mole for 3KCX or − 11.99 kcal/mole for 1E3G. Taking into consideration this threshold, the two plant species are more efficient against brain cancer than prostate cancer. The target amino-acids implicated in hydrogen bonds are given in Table 2.

Based only on the H-bonding interaction, this table shows that ligands **1** and **2** have a good pharmacophore profile to target both the 3KCX and 1E3G proteins. More importantly, it can be seen that all amino acids residues involving in the hydrogen bonding interaction in ligands **1** and **2** in the receptors sites are present in the co-crystalized binding site (PDB ligand).

Inspection of Table 3 shows that all ligands meet every single criterion of Lipinski's rule of five and thus fully obey the rule. Indeed, Lipinski's rules predict that the absorption of a compound is low when (1) the molecular weight is greater than 500; (2) the number of donor hydrogen bonds is greater than 5; (3) the number of acceptor hydrogen bonds is greater than 10; (4) the partition coefficient is greater than 5 (Lipinski 2000). The bioavailability score reveals that all four compounds virtually tested are orally bioavailable in rats (Martin 2005) and

can be absorbed in the intestine with respect to the TPS value ≤ 140 Å^2 (Clark 1999; Verber et al. 2002). However, only compound **3** is capable according to Hitchcock (2008) criteria of crossing the blood–brain barrier. As a result, they possess drug-like properties, of which only compound **3** fulfills the conditions for serving as a lead-like compound (Scheneider 2002). The partition coefficient, a physico-chemical parameter used to measure the tendency of a molecule to dissolve in membranes, which is correlated with its tendency to dissolve in an organic solvent, is inversely proportional to solubility. Thus, a Log *P* value that is too high will suggest that the molecule may be poorly soluble in an aqueous environment. The logarithm of partitioning coefficient between n-octanol and water phases ranges for 95% of existing drugs: − 2 to 6 (Ntie-Kang 2013). All the four compounds have a Log *P* comprising in this interval. These two physicochemical parameters (*P* and *S*) are related to the absorption of drugs in the organism. In the present study, the values of Log *S* (solubility) are between − 6.54 and − 3.78. Compound **2** has the best solubility (Log S $>$ − 4) while the other compounds are poorly soluble (Bergstrom et al. 2003).

It can also be noted that Log Kp values are within normal limits (between − 8 and − 1) indicating that these compounds are likely to be distributed in the organism for bio-transformation (Yadav et al. 2018).

Table 4 shows that compounds **1** and **2** are highly soluble and have the best absorption rate in the intestine. Only compounds **1** and **2** can serve as substrate for glycoprotein P, but all are inhibitors of this transmembrane protein. It is also noted that apart from compound **3**, all other compounds (**1**, **2** and **4**) have a VDss $<$ 0.45 (low). Only compound **3** (LogBB $>$ 0.3) can cross the blood–brain barrier, while the others can be moderately distributed in the brain (Log BB $<$ − 1). Compounds **3** and **4** can enter the CNS (Log PS $>$ − 2). None of these four compounds is metabolized by cytochrome P450 2D6 or its inhibitor. Compound **1** is an inhibitor of CYP3A4 while compounds **3** and **4** are its substrates. In addition, ligand **3** is an inhibitor of CYP1A2, CYP2C19 and, CYP2C9. The inhibition of CYP2C9 by compound **3** means that there is a possibility of interaction between the plant and NSAIDs/antiarrhythmics (amiodarone) and anticoagulants (acenocoumarol) because the latter are biotransformed by CYP2C9. Cytochrome P450 2C19 is involved in the bioactivation of pro-drugs into bio-active metabolites. Its inhibition by compound **3** would lead to a decrease in the activity of the pro-drugs. This is notably the case with clopidogrel, a platelet anti-aggregate used in acute coronary syndrome (Desmeules 2010). Of the above, only compound **4** has a good metabolic profile (P-gp inhibitor and CYP3A4 substrate), while the risk of interaction between compounds **1**, **2** and **3** is possible in individuals taking *D. quercina* herbal tea alone or when combined with drugs that are substrates for these enzymes. Indeed, the inhibition of P-gp and CYP3A4 by compound **1**, for example, will lead to the accumulation of compound **3**. A drug interaction is also possible between the four compounds when the phyto-drug is formulated from two plants (*D. quercina* and S. *leptoclada*).

Biochemically, various transmembrane proteins, such as P-glycoprotein (Pgp), CD243, or Multi-drug Resistance protein (MDR1), part of the ATB-Binding cassette (ABC) super family of transporter proteins, play an important role in the bioavailability of drugs. Indeed, several drug chemistry compounds can inhibit or induce ATPase P-gp activity, thus altering the kinetics of drug substrates for this transporter (Kale et al. 2012). Once distributed, these chemical compounds undergo biotransformation in the liver using P450 cytochromes (phase I) and other enzymes such as glutathione s-transferases (GST), catechol o-methyl transferase (COMT), or glucuro-nyltransferases (phase II: conjugations) that facilitate their elimination from the body (ADME process). In humans, the expression of detoxification genes (MDR1, Cytochrome P450) and therefore the response to drug treatment vary from one individual to another (Fattinger and Meier-Abt 2003). This inter-individual variation constitutes what is called "genetic polymorphism." Genetic polymorphism is a non-pathological variation in a nucleotide sequence between individuals due to a genetic mutation (Ameziane et al. 2006). This is the case in particular of the C3435 T mutation located in exon 26 of the MDR1 gene, whose CC genotype (high prevalence rate in negroids) is characterized by overexpression of P-gp, significant excretion (efflux) of substrates, and a low plasma level of substrates compared to the CT and TT genotypes (Caucasian populations). It is well established that P-gp substrates are also those of CYP3A4.

Indeed, an induction of CYP3A4 leads to an increase in P-gp expression as the genes encoding these two are located on chromosome 7 (P-gp: 7q21.1 and CYP3A4: 7q22.1) and would be regulated by the same mechanism (Feaz 2016).

In addition, it should be noted that P-gp limits the absorption of xenobiotic compounds from the gastrointestinal tract by promoting elimination in urine and bile but also participates in a protective barrier role for the CNS and the fetus (blood–brain and placental barrier).

After absorption and diffusion, five iso-enzymes (alternative forms) of cytochrome P450 (CYP1A2, CYP3A4, CYP2C9, CYP2C19, and CYP2D6) are involved in the metabolism (Phase I) of 50–90% of the drugs (Desmeules 2010). Clinically, their inhibition can decrease the elimination of the drug and increase its bioavailability,

resulting in an overdose that can be fatal for the patient. A drug interaction occurs when a given chemical compound inhibits the enzymatic activity of cytochrome P450, leading to the accumulation of its drug-substrate in the body. Table 4 also shows that compound 4 has a low clearance value, indicating that its concentration in the body is low. This means that its rate of elimination from the body is very high. This elimination is essentially metabolic. Only compound **3** can be eliminated via the organic cation transporter OCT2. Regarding the toxicological profile, only compound **1** is potentially mutagenic and hepatotoxic. However, none of the four compounds is cardio-toxic.

Conclusions

The search for new potential candidates for the treatment of breast and prostate cancers led us to carry out a computational study by molecular docking of four compounds from Malagasy medicinal plants to evaluate their antitumor potential in interaction with the angiogenesis target protein HIF-1α (3KCX) and human androgen receptor (1E3G), as well as to establish the pharmacokinetic profile of the four compounds. For 3KCX and 1E3G receptors, compounds **1**, **2**, and to some extent, compound **3,** were identified as having significant activity in inhibiting the receptors, with strong binding affinity on 1E3G receptor: − 10.08 kcal/mol (compound 1) compared to − 8.49 kcal/mol for the 3KCX receptor, for example. The pharmacokinetic profile of the three top compounds confirms that compounds **1** (1′,4-dihydroxy-2,3′-dimethyl-1,2′-binapthyl-5,5′,8,8′-tetraone) and **2** (6′-ethoxy-1′3′-dihydroxy-4,6-dimethyl-1,2′-binaphthyl-2,5′,8,8′-tetraone) can be considered hits since they are non-carcinogenic and non-hepatotoxic, and could thus be useful as alternative therapy in breast cancer than in prostate cancer. It is therefore desirable to determine the C-docker interaction energy and root mean square deviation (RMSD) of these compounds, to synthesize them in order to evaluate their in vivo antitumor effects on Ehrlich ascites carcinoma cells model.

Abbreviations

ADMET: Absorption, distribution, metabolism, excretion, and toxicity; BBB: Blood–brain barrier; BioS: Bioavailability score; CC genotype: Cytosine–cytosine genotype; CNS: Central nervous system; COMT: Catechol O-methyl transferase; CYP: Cytochrome; GST: Glutathione s-transferase; HAR: Human androgen receptor; HBA: Hydrogen bond acceptor; HBD: Hydrogen bond donor; HIF: Hypoxia-inducible factors; LC/MS/NMR: Liquid chromatography/mass spectroscopy/nuclear magnetic resonance; MDR1: Multi-drug resistance protein; MR: Molar refractivity; MW: Molecular weight; nRB: Number of the rotatable bonds; OCT: Organic cation transporter; PDB: Protein Data Bank; P-gp: P-glucoprotein; RMS: Root mean square; TSA: Topological surface area; VD: Volume distribution; WHO: World Health Organization.

Acknowledgements

Not applicable.

Author contributions

J.P.K.N.N., F.P.R., and R.B. involved in research concept and design, J.T.K., A.M., and C.M.A. took part in collection and/or assembly of data, J.P.K.N.N., J.T.K., and A.M. involved in data analysis and interpretation, J.P.K.N.N., P.T.M., and V.M. took part in writing the article, and J.P.K.N.N., J.M., and C.M.N. involved in critical revision of the article. All authors have read and approved the manuscript.

Funding

No funding received for this study.

Availability of data and materials

These are available from the corresponding author on reasonable request.

Declarations

Ethics approval and consent to participate

Not applicable.

Consent for publication

Not applicable.

Competing interests

The authors declare that there is no conflict of interests regarding the publication of this paper.

Author details

[1]Department of Basic Sciences, Faculty of Medicine, University of Gbado-Lite, Gbado-Lite, Nord-Ubangi Province, Democratic Republic of the Congo. [2]Department of Biology, Faculty of Science, University of Kinshasa, Kinshasa, Democratic Republic of the Congo. [3]Department of Chemistry, Faculty of Science, University of Kinshasa, Kinshasa, Democratic Republic of the Congo. [4]School of Education, College of Education, University of Rwanda, Kigali, Rwanda. [5]Department of Basic Sciences, Faculty of Medicine, University of Kinshasa, Kinshasa, Democratic Republic of the Congo. [6]Department of Organic Chemistry, University of Toliara, Toliara, Madagascar. [7]Antananarivo Poly-Technique High School, University of Antananarivo, Antananarivo, Madagascar.

Received: 22 January 2022 Accepted: 3 April 2022
Published online: 13 April 2022

References

Alamri MA (2020) Pharmaco-informatics and molecular dynamic simulation studies to identify potential small-molecule inhibitors of WNK-SPAK/OSR1 signaling that mimic the RFQV motifs of WNK kinases. Arab J Chem 13:5107–5117. https://doi.org/10.1016/j.arabjc.2020.02.010

Ameziane N, Bogard M, Lamoril J (2006) Principes de biologie moléculaire en biologie clinique. Elsevier SAS, Paris (**ISBN: 2-84299-685-2**)

Anshika NS, Meghna MB, Neeti S (2017) Structure Based docking studies towards exploring potential anti-androgen activity of selected phytochemicals against prostate cancer. Sci Rep 7:1955. https://doi.org/10.1038/s41598-017-02023-5

Ashfaq UA, Mumtaz A, ul Qamar T, Fatima T (2013) MAPS database: medicinal plant activities, phytochemical and structural database. Bioinformation 9:993. https://doi.org/10.6026/97320630009993

Bergstrom CAS, Strafford M, Lazorova L, Avdeef A, Luthman K, Per A (2003) Absorption classification of oral drugs based on molecular surface properties. J Med Chem 46:558–570. https://doi.org/10.1021/jm020986i

Clark DE (1999) Rapid calculation of polar molecular surface area and its application to the prediction of transport phenomena. 2. Prediction of blood–brain barrier penetration. J Pharm Sci 88:815–821. https://doi.org/10.1021/js980402t

Daina A, Olivier M, Zoete V (2017) SwissADME: a free web tool to evaluate pharmacokinetics, druglikeness and medicinal chemistry friendliness of small molecules. Sci Rep 7:42717. https://doi.org/10.1038/srep42717

Desmeules J (2010) Importance des cytochromes P450: pharmacogénétique et interactions médicamenteuses. J Med Chem 37:7–10

Dufrasne F, Gelbcke M, Nève J, Kiss R, Kraus J-L (2011) Quinone methides and their prodrugs: a subtle equilibrium between cancer promotion, prevention, and cure. Curr Med Chem 18:3995–4011

Fatiany PR, Robijaona B, Randrianarivo E, Raharisololalao A, Martin MT, Ngbolua KN (2013) Antiplasmodial and cytotoxic activities of triterpenic quinone isolated from a medicinal plant species *Salacia leptoclada* Tul. (Celastraceae) originate to Madagascar. Asian Pac J Trop Biomed 3:780–784. https://doi.org/10.1016/S2221-1691(13)60155-0

Fatiany PR, Robijaona B, Randrianarivo E, Raharisololalao A, Martin MT, Ngbolua KN (2014) Isolation and structural elucidation of cytotoxic compounds from *Diospyros quercina* (Baill.) endemic to Madagascar. Asian Pac J Trop Biomed 4:169–175. https://doi.org/10.1016/S2221-1691(14)60227-6

Fattinger K, Meier-Abt A (2003) Interactions entre phytothérapie et médicaments. Forum Med Suisse 29:693–700

Feaz L (2016) Rôle de la glycoprotéine P dans les interactions médicamenteuses au niveau de la Barrière hémato-encéphalique: données de la pharmacovigilance française. Sciences pharmaceutiques. Dumas-0159824. https://dumas.ccsd.cnrs.fr/dumas-01598244

Genheden S, Ryde U (2015) The MM/PBSA and MM/GBSA methods to estimate ligand-binding affinities. Expert Opin Drug Discov 10:449–461. https://doi.org/10.1517/17460441.2015.1032936

Gothié E, Pouysségur J (2002) HIF-1: Régulateur central de l'hypoxie. Med Sci 18:70–78. https://doi.org/10.1051/medsci/200218170

Hernandes C, Miguita L, Oliveira de Sales R et al (2020) Anticancer activities of the quinone-methide triterpenes maytenin and 22-_-hydroxymaytenin obtained from cultivated Maytenus ilicifolia roots associated with down-regulation of miRNA-27a and miR-20a/miR-17-5p. Molecules 25:760–778. https://doi.org/10.3390/molecules25030760

Hitchcock SA (2008) Blood–brain barrier permeability considerations for CNS-targeted compound library design. Curr Opin Chem Biol 12:318–323. https://doi.org/10.1016/j.cbpa.2008.03.019

Hollingsworth SA, Dror RO (2018) Molecular dynamics simulation for all. Neuron 99:1129–1143. https://doi.org/10.1016/j.neuron.2018.08.011

Hopkins AL, Groom CR, Alex A (2004) Ligand efficiency: a useful metric for lead selection. Drug Discov Today 9:430–431. https://doi.org/10.1016/S1359-6446(04)03069-7

Iteku BJ, Mbayi O, Bongo NG, Mutwale KP, Wambale JM, Lengbiye E, Ngunde Ngunde S, Ngbolua KN (2019) Phytochemical analysis and assessment of antibacterial and antioxidant activities of Phytolacca dodecandra L. Herit leaf extracts (Phytolaccaceae). Int J Biomed Eng Clin Sci 5:31–39. https://doi.org/10.11648/j.ijbecs.20190503.11

Kale M, Raghava S, Lakshmi PK (2012) Overview of P-glycoprotein inhibitors: a rational outlook. Braz J Pharm Sc 48:353–367. https://doi.org/10.1590/S1984-82502012000300002

Kasende OE, Matondo A, Muya JT, Scheiner S (2017) Interactions between temozolomide and guanine and its S and Se-substituted analogues. Int J Quantum Chem 117:157–169. https://doi.org/10.1002/qua.25294

Lipinski CA (2000) Drug-like properties and the cause of poor solubility and poor permeability. J Pharmacol Toxicol Methods 44:235–249. https://doi.org/10.1016/s1056-8719(00)00107-6

Lonergan EP, Tindall JD (2011) Androgen receptor signaling in prostate cancer development and progression. J Carcinog 10:20. https://doi.org/10.4103/1477-3163.83937

Martin YC (2005) A bioavailability score. J Med Chem 48:3164–3170. https://doi.org/10.1021/jm0492002

Matondo A, Kilembe JT, Mwanangombo DT, Nsimba BM, Mawete DT, Gbolo BZ, Bongo GN, Ngbolua KN (2020) Facing COVID-19 via anti-inflammatory mechanism of action: molecular docking and pharmacokinetic studies of six-anti-inflammatory compounds derived from *Passiflora edulis*. J Complet Altern Med Res 12:35–51. https://doi.org/10.9734/jocamr/2020/v12i330211?

Matondo A, Kilembe JT, Ngoyi EM, Kabengele CN, Kasiama GN, Lengbiye EM, Mbadiko CM, Inkoto CL, Bongo GN, Gbolo BZ, Falanga CM, Mwanangombo DT, Opota DO, Tshibangu DST, Tshilanda DD, Ngbolua DD, Mpiana PT (2021) Oleanolic acid, ursolic acid and apigenin from *Ocimum basilicum* as potential inhibitors of the SARS-CoV-2 main protease: a molecular docking study. Int J Pathog Res 6:1–16. https://doi.org/10.9734/ijpr/2021/v6i230156

Morris GM, Goodsell DS, Halliday RS, Huey R, Hart WE, Belew RK, Olson AJ (1998) Automated docking using a Lamarckian genetic algorithm and empirical binding free energy function. J Comput Chem 19:1639–1662. https://doi.org/10.1002/(SICI)1096-987X(19981115)19:14%3c1639::AID-JCC10%3e3.0.CO;2-B

Mpiana PT, Ngbolua KN, Tshibangu DST, Kilembe JT, Gbolob BZ, Mwanangombo DT, Inkoto LC, Lengbiye ME, Mbadiko MC, Matondo A, Bongo NG, Tshilanda DD (2020) Identification of potential inhibitors of SARS-CoV-2 main protease from *Aloe* vera compounds: a molecular docking study. Chem Phys Lett 754:137751. https://doi.org/10.1016/j.cplett.2020.137751

Ngbolua KN, Rafatro H, Rakotoarimanana H, Ratsimamanga US, Mudogo V, Mpiana PT, Tshibangu DST (2011a) Pharmacological screening of some traditionally-used antimalarial plants from the Democratic Republic of Congo compared to its ecological taxonomic equivalence in Madagascar. Int J Biol Chem Sci 5:1797–1804. https://doi.org/10.4314/ijbcs.v5i5.3

Ngbolua KN, Rakotoarimanana H, Rafatro H, Ratsimamanga US, Mudogo V, Mpiana PT, Tshibangu DST (2011b) Comparative antimalarial and cytotoxic activities of two Vernonia species: V. amygdalina from the Democratic Republic of Congo and V. cinerea subsp vialis endemic to Madagascar. Int J Biol Chem Sci 5:345–353. https://doi.org/10.4314/ijbcs.v5i1.68111

Ngbolua KN, Tshibangu DST, Mpiana PT, Mudogo V, Tshilanda DD, Masengo AC, Selvaraj D, Muthiah R, Govindarajan S (2018) Medicinal plants from Democratic Republic of the Congo as sources of anticancer drugs. J Adv Botany Zool. https://doi.org/10.5281/zenodo.1162973

Nirmala GSG, Varsha DS, Samudyata CP, Sunanda T, Saravana BC, Prasanna KS (2022) Ehrlich Ascites carcinoma mice model for studying liver inflammation and fibrosis. Adv Cancer Biol. https://doi.org/10.1016/j.adcanc.2022.100029

Nissink JWM, Murray C, Hartshorn M, Verdonk ML, Cole JC, Taylor R (2002) A new test set for validating predictions of protein-ligand interaction. Proteins Struct Funct Genet 471:457–471. https://doi.org/10.1002/prot.10232

Ntie-Kang F (2013) An in silico evaluation of the ADMET profile of the StreptomeDB database. Springerplus 2:353. https://doi.org/10.1186/2193-1801-2-353

Pezzuto A, Carico E (2018) Role of HIF-1 in cancer progression: novel insights, a review. Curr Mol Med 18:343–351. https://doi.org/10.2174/1566524018666181109121849

Scheneider G (2002) Trends in virtual computational library design. Curr Med Chem 9:2095–2102. https://doi.org/10.2174/0929867023368755

Selvaraj A, Antony S, Hakdong S (2019) Anti-methanogenic effect of rhubarb (Rheum spp.)-An in silico docking studies on methyl-coenzyme M reductase (MCR). Saudi J Biol Sci 26:1458–1462. https://doi.org/10.1016/j.sjbs.2019.06.008

Shapovalov MS, Dunbrack RL (2011) A smoothed backbone-dependent rotamer library for proteins derived from adaptive kernel density estimates and regressions. Structure 19:844–858. https://doi.org/10.1016/j.str.2011.03.019

Siegel RL, Miller KD, Jemal A (2019) Cancer statistics. Cancer J Clin 69:7–34

Trott O, Olson AJ (2010) AutoDock Vina: improving the speed and accuracy of docking with a new scoring function, efficient optimization, and multithreading. J Comput Chem 31:455–461. https://doi.org/10.1002/jcc.21334

Tshibangu DST, Selvaraj D, Muthiah R, Govindarajan S, Ngbolua KN, Mudogo V, Tshilanda DD, Misengabu MN, Mpiana PT (2016a) *In Vitro* anticancer assessment of Annickia chlorantha (Oliv.) Setten & Maas Stem (Annonaceae) Bark from Democratic Republic of Congo. J Biosci Med 4:23–29. https://doi.org/10.4236/jbm.2016.44004

Tshibangu DST, Selvaraj D, Muthiah R, Syamala G, Ngbolua KN, Mudogo V, Tshilanda DD, Gbolo ZB, Mpiana PT (2016b) *In vitro* screening of the leaf extracts from Gardenia ternifolia (Forest Gardenia) for their anticancer activity. J Compl Altern Med Res 1:1–7. https://doi.org/10.9734/JOCAMR/2016/28348

Tshilanda DD, Inkoto LC, Kashala M, Mata S, Mutwale KP, Tshibangu DST, Bongo NG, Ngbolua KN, Mpiana PT (2019) Microscopic studies, phytochemical and biological screenings of *Ocimum canum*. Int J Pharm Chem 5:61–67. https://doi.org/10.11648/j.ijpc.20190505.13

Tunga KA, Kilembe JT, Matondo A et al (2020) Computational analysis by molecular docking of thirty alkaloid compounds from medicinal plants as potent inhibitors of SARS-CoV-2 main protease. Res Square. https://doi.org/10.21203/rs.3.rs-94752/v1

Verber DF, Johnson SR, Cheng HY, Smith BR, Ward KW, Kopple KD (2002) Molecular properties that influence the oral bioavailability of drug candidate. J Med Chem 45:2615–2623. https://doi.org/10.1021/jm020017n

Vidya M, Madhu SS, Batoul F, Mastan M, Afroz A, Ganj PN (2019) Molecular docking of angiogenesis target protein HIF-1α and genistein in breast cancer. Genetics 701:169–172. https://doi.org/10.1016/j.gene.2019.03.062
Yadav DK, Kumar S, Saloni MS, Yadav L, Teli M et al (2018) Molecular insights into the interaction of RONS and Tieno [3,2-C] pyran analogs with SIRT6/COX-2: a molecular dynamics study. Sci Rep 8:4777. https://doi.org/10.1038/s41598-018-22972-9

Publisher's Note